Masses of Black Holes in Active Galactic Nuclei: Implications for NLS1s (invited)

Bradley M. Peterson[*]

Deparment of Astronomy and Center for Cosmology and AstroParticle Physics, The Ohio State University
E-mail: peterson@astronomy.ohio-state.edu

I review how AGN black hole masses are calculated from emission-line reverberation-mapping data, with particular attention to both assumptions and caveats. I discuss the empirical relationship between AGN luminosity and broad-line region radius that underpins the indirect methods by which most AGN masses are estimated. I also discuss how line widths are characterized in this method and illustrate how different ways of measuring the line-widths can lead to systematic errors in the mass scale. I discuss specific implications for NLS1 galaxies and consider whether the NLS1 phenomenon is better explained by source inclination or by Eddington rate, and conclude that there is evidence that *both* of these effects are contributing factors and that at least the high-Eddington rate NLS1s are physically similar to some high-luminosity quasars.

---

[*]Speaker.

1. Introduction

The masses of black holes in the nuclei of galaxies are measured by observing how they accelerate test masses in their vicinity, as is always the case in astronomy. The "test masses" in the case of galactic nuclei are stars or gas in the nuclear regions. The particular advantage of using stars as the test masses around black holes is that they are subject only to gravitational forces. Unfortunately, stellar dynamics can be modeled accurately only with high angular-resolution spectroscopy; the black hole radius of influence,

$$R_{\mathrm{BH}} = 2GM_{\mathrm{BH}}/\sigma_*^2, \tag{1.1}$$

where σ_* is the stellar velocity dispersion of the host galaxy bulge, must be resolved, or at least nearly so. Measurements of gas motions, on the other hand, allow us to probe much closer to the black hole, on scales far below the black hole radius of influence in the case of reverberation mapping [15, 76]. However, gas also responds to non-gravitational forces, such as hydromagnetic acceleration and radiation pressure, which must be accounted for.

Methods that rely on measurements of the motions of stars or gas that are accelerated by the black hole are "direct methods." These include modeling of both stellar and gas dynamics and reverberation mapping. We also employ "indirect methods" of mass determination that measure observables that are *correlated* with black hole mass: these include the relationships between black hole mass and stellar bulge velocity dispersion (the M_{BH}–σ_* relationship [34, 38, 44]), black hole mass and host-galaxy bulge luminosity (the M_{BH}–L_{bulge} relationship, which is also sometimes known as the Magorrian [61] relationship), the fundamental plane, and AGN-specific relationships, such as that between the AGN luminosity and the size of the broad-line region (BLR), as discussed below and by Bentz [5]. It is also useful to distinguish among "primary," "secondary," and "tertiary" methods of mass determination: primary methods are those that require the fewest assumptions. Certainly, in the case of supermassive black holes, mass measurements based on the proper motions and radial velocities (Sgr A*) or megamasers (NGC 4258) are primary. Also generally regarded as primary in the measurement of nuclear supermassive black holes are stellar and gas dynamics. Reverberation mapping, however, as it is currently practiced, requires an external calibration of the zero-point for its mass scale through correlations between the black hole mass and host-galaxy properties that are assumed to be the same for the host galaxies of active and quiescent black holes; for this reason reverberation mapping is a "secondary method," although it is still a "direct method." However, as discussed below, reverberation mapping has the potential to become a primary method. Since it will be the only method that is potentially extendable to high redshift and the method most applicable to NLS1s, it will be the main focus of the rest of this contribution.

2. Results from Reverberation Mapping

The desired outcome of reverberation mapping is usually expressed in terms of a "velocity–delay map" (also called the "transfer function" [15]) $\Psi(\tau, V_{\mathrm{LOS}})$ which is the six-dimensional phase space of the BLR (velocity field and geometry) projected into the two observables, time delay τ and line-of-sight (i.e., Doppler) velocity V_{LOS}. The data requirements for successful recovery of $\Psi(\tau, V_{\mathrm{LOS}})$ from spectrophotometric monitoring are fairly stringent [47] and it is therefore only recently that high-quality maps are starting to appear [14, 30]. It is much more common to extract

only the mean response time for an emission line integrated over all Doppler velocities. Simple cross-correlation of the continuum and emission-line light curves gives a mean response time for a particular emission line, and this mean response time is weighted toward physical conditions where both the emissivity and responsivity (marginal change in emissivity in response to a continuum change) are high. Even in this simplified analysis, advances continue to be made as improved mathematical descriptions of AGN variability [53, 60] have led to more observationally motivated statistical modeling of the continuum behavior in the gaps in coverage in the real time-series sampling. Recent improvements in this methodology [104] allow self-consistent determination of the uncertainties and, since multiple lines with different lags can be dealt with simultaneously, make it possible to back-fill some of the gaps in time series. The new methodology yields lags that are largely consistent with those based on current cross-correlation practices, but with reduced uncertainties in the lag measurements and, indeed, more robust estimates of these uncertainties.

At the time of this workshop, reverberation lag measurements have been made for around 50 AGNs. Since the compilation of Peterson et al. [82], there have been new reverberation results from MDM Observatory and Crimean Astrophysical Observatory [7, 8, 25, 27, 28, 29, 42, 43], the Lick AGN Monitoring Program (LAMP) [9, 12, 13, 14, 3] and other programs [88, 91] that have concentrated primarily on the Balmer lines in low-redshift AGNs. There have also been new measurements of the C IV λ1549 response in the dwarf Seyfert NGC 4395 [83] and in one high-redshift quasar [52]. The Mg II λ2798 response has been measured reliably in only one case, NGC 4151 [69].

The major conclusions that can be drawn from these studies are:

1. Different emission lines respond on different time scales, with lines characteristic of the highest ionization gas responding first, providing evidence for ionization stratification of the BLR. The size of the BLR, as measured by a particular emission-line time delay τ, is inferred to be $R_{\mathrm{BLR}} = c\tau$.

2. In every case where the time delays for multiple broad emission lines have been measured [77, 78, 58, 13] there is a tight anticorrelation between line width ΔV and time lag τ such that the product $\Delta V^2 \tau$ is constant (Figure 1), as expected if the dynamics of the BLR is dominated by the gravitational potential of the central black hole. Strictly speaking, it means that the BLR gas is responding to an inverse-square force or forces, so radiation pressure might also play a role [62] (see Marconi's contribution to these proceedings for a more thorough discussion [63]).

3. The time lag for the emission-line response to continuum variations is longer in more luminous objects [50, 51]. After separating the AGN luminosity L_{AGN} from the starlight contamination by the host galaxy [6, 11], the relationship between these quantities is consistent with $R_{\mathrm{BLR}} \propto L_{\mathrm{AGN}}^{1/2}$. This is well-established only for Hβ, but the more limited reverberation results for C IV [82, 83, 52] are consistent with the same relationship. This radius–luminosity (*R–L*) relationship provides the underpinning for indirect methods of measuring AGN black-hole masses over cosmic time [5, 95].

4. In every case in which the response of a particular emission line has been measured on multiple occasions, the timescale for response of the emission line is consistent with $\tau \propto L_{\mathrm{UV}}^{1/2}$,
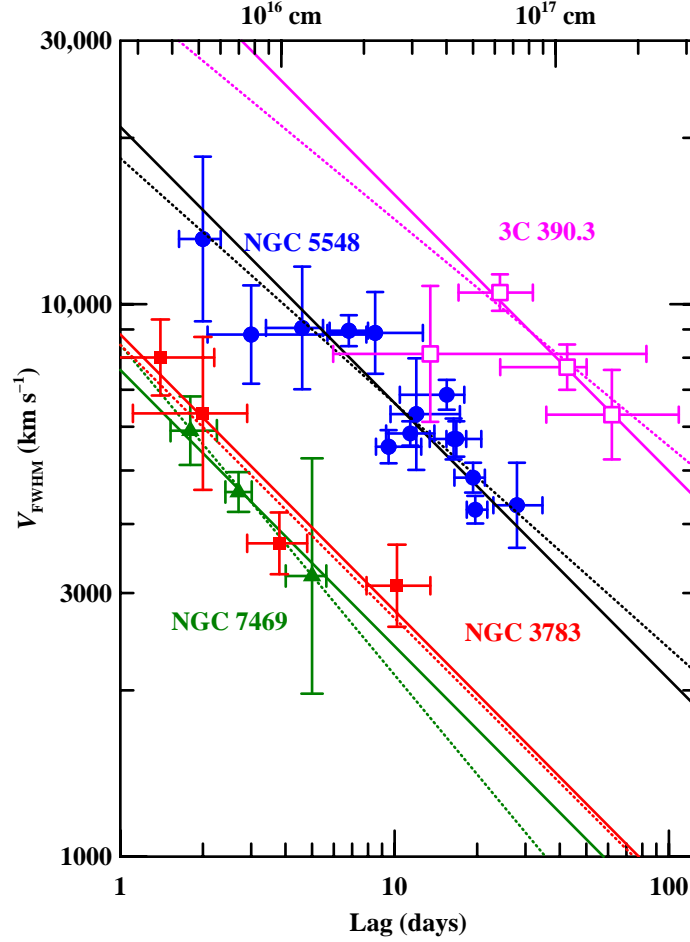
Figure 1: Line-width vs. emission-line lag (in days) for four reverberation-mapped AGNs. In each case, the data are consistent with a virial relationship, i.e., $V \propto \tau^{-1/2}$. The dotted lines are show the best-fit slopes and the solid lines show the best-fit virial relationship [77, 78].

where L_{UV} is the luminosity in the observable UV, as close to the ionizing continuum as possible [81]. The emission-line width also changes in a way that is at least approximately consistent with a constant value of the product $\Delta V^2 \tau$.

It is worth mentioning that the strong optical Fe II blends that are prominent features of Seyfert 1 spectra are seen to vary over time scales that are long compared to reverberation time scales, but do not appear to vary much if at all on reverberation time scales [96, 57]. This may be because the emissivity and responsivity distributions for these lines are not highly localized, as they seem to be in the case of most of the prominent emission lines in AGNs. In other words, these features *vary*, but they do not *reverberate*.

Results (2) and (4) above suggest that we can measure the central black hole mass by combining the emission-line width ΔV and time lag τ, i.e.,

$$M_{BH} = f \left(\frac{\Delta V^2 c \tau}{G} \right).$$

(2.1)

The quantity in parentheses is based on the observable quantities and has units of mass; we refer to it as the "virial product." The factor f is a dimensionless number of order unity into which we subsume all of our ignorance of about the geometry and kinematics of the BLR; what we are attempting to do is to characterize a probably complex BLR with two observables that we hope will somehow average over the complexity well enough to yield a reasonable mass estimate. Let's consider the elements of this equation individually:

- As noted earlier, τ is the mean time lag for a given emission line. Practically speaking, it is usually the centroid of the continuum/emission-line cross-correlation function. It is unbiased as a function of BLR inclination as long as the BLR is axisymmetric and emits isotropically (and even when it does not emit isotropically, the correction factor is relatively small compared to other projection effects).

- The line width ΔV is more problematic, as there are multiple issues to consider. The first of these is what line-width measure to use? Commonly used measures are (a) full-width at half maximum (FWHM) and (b) line dispersion σ_{line}, the second moment of the line profile. Both measures have liabilities: FWHM is more sensitive to both random noise, unremoved narrow-line components, and absorption due to intervening gas (at least in the case of resonance lines like C IV $\lambda 1549$) and σ_{line} is more sensitive to blending with other features[1]. Second, given an array of spectra from a reverberation-mapping monitoring campaign, we have two obvious alternatives for forming the spectrum from which we measure the line widths. The first of these is the mean spectrum, which we construct by determining the average flux in each wavelength bin of the spectrum over the duration of the monitoring campaign. The second of these is an "rms spectrum" that is comprised of the root-mean-square fluxes in each wavelength bin of the spectrum over the duration of the campaign. The rms spectrum affords two particular (related) advantages: (a) the rms spectrum isolates the emission-line gas that is actually responding to the continuum variations and omits the unchanging parts (thus automatically excluding narrow-line components and host-galaxy starlight), and (b) we find in practice that the variable parts of the emission lines are much less blended with other features, mostly because some features such as the optical Fe II lines do not vary on reverberation time scales, but partly because the widths of the emission lines are typically narrower in the rms spectrum than in the mean spectrum (possibly because the very highest velocity BLR gas is optically thin [33, 89]). A nice comparison of a mean and an rms spectrum is shown in Grier et al.'s contribution to these proceedings [43].

- The scaling factor f converts the convenient virial product, based on the observables, to an actual mass. If the BLR is a flat Keplerian disk observed at inclination i, the scaling factor would include a $1/\sin^2 i$ term to account for the velocity projection. It could also include a correction factor for τ if the line emission is anisotropic. Also — and this is a critical point that is often misunderstood — the value of f depends on what line-width measure is being used. This is an extremely important point that I will return to below.

---

[1]We are currently experimenting with using interpercentile widths [100] as an alternative characterization of line width, as have Fine et al. [36], but it is premature to conclude anything at this point.

Table 1: Black Hole Masses (Units of $10^6 M_\odot$)

Galaxy	NGC 3227	NGC 4151
Direct methods:		
Stellar dynamics	7–20 [23]	< 70 [73]
Gas dynamics	20^{+10}_{-4} [46]	$30^{+7.5}_{-22}$ [46]
Reverberation	7.63 ± 1.7 [29]	46 ± 5 [7]
Indirect methods:		
$M_{\rm BH}$–σ_*	25	6.1
R–L scaling	15	65

It should be clear from this discussion that the scale factor f is different for every AGN; indeed, in principle it could be somewhat different for different emission lines in the same AGN, but not too much different since, as shown in Figure 1, the virial product is approximately constant for all emission lines. Without additional information on the kinematics, geometry, and inclination of the AGN, we cannot determine f for a particular source.

We could also determine f if we had an independent measure of the black hole mass. Unfortunately, there are very few cases where alternative direct measurements exist (see below), and none of these are high precision measurements. We can, however, use other *indirect* methods to estimate the black hole masses in reverberation-mapped AGNs and use these to determine the scale factor. However, since the fidelity of individual mass measurements by indirect methods is low, we can realistically hope to obtain only a mean value $\langle f \rangle$ for the reverberation-mapped sample and thus effect a statistical scale factor for the reverberation-mapped sample. This has been done by assuming that the $M_{\rm BH}$–σ_* relationship for AGNs is the same as it is in quiescent galaxies. It is well-known that reverberation-based black hole masses scale with stellar bulge velocity dispersion in a fashion similar to that seen in quiescent galaxies [39, 35, 72, 70, 103] so it is not too much of a stretch to assume that the zero-points for the AGN and quiescent-galaxy are identical. The most recent analysis gives a value of $\langle f \rangle = 5.25 \pm 1.21$ [103] (though see [40] and §4.3). The scatter around the AGN $M_{\rm BH}$–σ_* relationship is estimated to be ~ 0.4 dex, which is thus an estimate of the typical uncertainties in reverberation-based masses, assuming that the intrinsic scatter in the $M_{\rm BH}$–σ_* relationship is much smaller than this (but more on this later).

The reverberation-based black hole masses in the literature are computed from equation (2.1) with ΔV taken to be the line dispersion in the rms spectrum, τ is the cross-correlation centroid, and f is the value based on the $M_{\rm BH}$–σ_* relationship [72, 103]. In a small number of cases, we can compare the reverberation-based masses with those from other direct methods. Two cases are shown in Table 1, NGC 3227 and NGC 4151. In both cases, the direct methods are in reasonable agreement, particularly considering the factor of three or so systematic uncertainty in the reverberation-based masses and probably comparable systematic uncertainties in the other primary methods. Another check on the accuracy of reverberation-based masses is to compare the $M_{\rm BH}$–$L_{\rm bulge}$ relationship for AGNs to that for quiescent galaxies [10]. The agreement is found to be very good.

Use of a mean value $\langle f \rangle$ averages over the specific values of f for individual sources: if it is unbiased, $\langle f \rangle$ will result in equal numbers of mass overestimates and underestimates, but *these will*

not be a function of either time delay or line width.

3. Indirect Mass Measurements Anchored by Reverberation Mapping

As noted above (result 3 in the last section), reverberation mapping has revealed a tight relationship between the AGN continuum luminosity and the radius of the BLR [5] of the form

$$R_{\mathrm{BLR}} \propto L_{\mathrm{AGN}}^{\alpha}, \tag{3.1}$$

where empirically we find $\alpha \approx 0.5$, which is, as is often noted, consistent with the theoretical expectation. In the early days of photoionization equilibrium modeling of the BLR, Davidson [21] and others began to recognize that photoionization models could be parameterized by (a) the shape of the ionizing continuum, (b) the elemental abundances, (c) the particle density n_{H} and column density of the photoionized gas, and (d) an ionization parameter defined by

$$U = \frac{Q(\mathrm{H})}{4\pi R^2 c n_{\mathrm{H}}}, \tag{3.2}$$

where R is the separation between the source of ionizing photons and the photoionized gas (i.e., the BLR radius) and $Q(\mathrm{H})$ is the number of ionizing photons produced per second by the photoionizing source, i.e.,

$$Q(\mathrm{H}) = \int \frac{L_\nu}{h\nu} d\nu \tag{3.3}$$

and the integral is over all hydrogen-ionizing frequencies. To some low-order of approximation, AGN spectra are self-similar over many orders of magnitude in luminosity, which suggests that the BLRs of all AGNs are characterized by similar values of U and n_{H}. This leads to the prediction that

$$R_{\mathrm{BLR}} = \left(\frac{Q(\mathrm{H})}{4\pi c n_{\mathrm{H}} U} \right)^{1/2} \propto L_{\mathrm{AGN}}^{1/2}, \tag{3.4}$$

if we can use L_{AGN}, the luminosity at some observable wavelength, as a proxy for the ionizing luminosity. We characterize this expectation as "naïve" since some of the implicit assumptions are quite approximate: we know that the shape of the ionizing continuum should change with black hole mass and that the BLR is complex and cannot be characterized by fixed values of U and n_{H} [2, 55]. In the early photoionization equilibrium calculations in the 1970s, the size of the BLR was not considered to be an important parameter as the models suggested that the BLR sizes in quasars would range from one to a thousand light years or so [56, 22], which would be unresolvable in distant quasars in any event. I suspect that Davidson does not get enough credit for his insight on the ionization parameter and the R–L scaling relationship that follows from it because he wrote the ionization parameter in terms of the ionizing flux ($U \propto F_{\mathrm{ion}}/n_{\mathrm{H}}$) rather than the ionizing luminosity ($U \propto L_{\mathrm{ion}}/R^2 n_{\mathrm{H}}$), as it was written later [67], so the BLR radius did not appear explicitly. Nevertheless, the prediction of the R–L relationship was so well-known that a decade later it was often quoted without attribution (e.g., [64]) when the BLR size became an interesting parameter because the first emission-line variability studies suggested that the BLR was much smaller than predicted by the photoionization equilibrium models [79]. The R–L relationship was looked for as a prediction of photoionization theory even when the first crude reverberation

lags were measured [54]; it was always understood, of course, that the central mass could be easily estimated from a single quasar spectrum via equation (2.1) by using R_{BLR} from the R–L relationship and ΔV from an emission-line width measurement. This "photoionization method" [98, 50] thus provides a significant shortcut to estimating AGN black hole masses[2]. The general methodology has been extended to other emission lines, in particular, C IV $\lambda 1549$ [93, 94, 97] and Mg II $\lambda 2798$ [68]. Similar R–L relationships using various proxies for the continuum luminosity have also been shown to be viable [41].

The bottom rows of Table 1 show two indirect measurements of the black hole masses in NGC 3227 and NGC 4151. The indirect methods are in good agreement with the direct methods in the case of NGC 3227, but not quite as good in the case of NGC 4151. But generally the picture holds together to an accuracy of $\sim 0.5\,\mathrm{dex}$.

4. Implications for NLS1s

4.1 Inclination or Eddington Ratio?

There are two competing explanations for the properties of NLS1s:

1. NLS1s might be low-inclination sources, viewed nearly pole-on. If the broad-line emission arises primarily in a rotating Keplerian disk, for example, the projected rotational speed is decreased by a factor of $\sin i$, thus accounting for the unusually narrow broad lines.

2. NLS1s might be AGNs that are accreting at relatively high Eddington ratio: for a given luminosity, objects with the narrowest emission lines have the lowest black hole mass.

There is certainly evidence that in general broad lines widths are affected by inclination. The widths of the Balmer lines in core-dominated radio sources (those at low inclination) are systematically lower than those in the spectra of lobe-dominated (high-inclination) sources [102]. Similarly, radio sources with flat spectral indices (low inclination sources) have narrower line widths than radio sources with steep spectral indices [49]. Of course, the fact that "broad" lines are never narrower than $\sim 1000\,\mathrm{km\,s^{-1}}$ means that there must an an axial component to the BLR velocity field, but it still seems that the dominant motion might be rotational. Decarli et al. [24] make a good case that such a model can explain many of the properties of NLS1s, although I don't believe inclination can explain everything. Also, absorption-line and reverberation studies [19, 30] both suggest that the well-known NLS1 NGC 4051 is indeed observed at low-inclination. And, very importantly, some NLS1s have now been detected in very high energies by *Fermi* ([1, 37], suggesting that we are looking down the axis of these systems.

Is inclination sufficient to account for the NLS1 phenomenon? Probably not, in my opinion. I'll cite two specific examples. One of the few radio-loud reverberation mapped AGNs is 3C 120,

---

[2]This method for estimating quasar masses has been sometimes, misleadingly in my opinion, referred to as the "Dibai method" [16]. Dibai [31] noted that since AGN emission lines have the same equivalent widths regardless of luminosity $L_{\mathrm{line}} \propto L_{\mathrm{continuum}}$. If one then assumes constant emission-line emissivity per unit volume ε, then $L_{\mathrm{line}} = \varepsilon 4\pi R_{\mathrm{BLR}}^3/3$, or $R_{\mathrm{BLR}} \propto L_{\mathrm{cont}}^{1/3}$ and $M_{\mathrm{BH}} \propto \Delta V^2 L_{\mathrm{cont}}^{1/3}$. So while the predicted sizes for the BLRs in nearby AGNs were reasonable, the physics is incorrect and the functional form of the R–L relationship is wrong. Certainly Dibai did a lot of important work that was admittedly often overlooked in the West, but this incorrect attribution overlooks the more correct physical insights provided by Kris Davidson, Gordon MacAlpine, Chris McKee, Bruce Tarter, and others.

Table 2: Black Hole Mass Measurements for Mrk 110

Method	Mass (Units of $10^6 M_\odot$)
Reverberation:	25 ± 6
$M_{\mathrm{BH}}-\sigma_*$:	4.8
Gravitational redshift:	14 ± 3

which has a relativistic jet with an inclination $i < 20^\circ$. The inclination correction to the mass is at least a factor of 10 for this inclination; but 3C 120 nevertheless falls right on the $M_{\mathrm{BH}}-\sigma_*$ relationship rather than below it. Mrk 110 is another interesting case, an NLS1 with an independent black hole mass measurement based on the gravitational redshift of the emission lines [59]. As seen in Table 2, the reverberation mass is the largest of the three available mass estimates: we would expect it to be the *smallest* if the narrowness of the Balmer lines is attributable to inclination only as the other two measures should be independent of inclination.

Consider now the alternative explanation, that the NLS1 phenomenon is a manifestation of low black-hole mass at a given luminosity. Figure 2a shows the mass–luminosity relationship for reverberation-mapped AGNs, with the NLS1s highlighted. The NLS1s are generally high Eddington ratio (i.e, accretion rate relative to the Eddington value) objects, but they are also generally low-luminosity sources. This, we shall see, is an accident of how the NLS1 class was defined.

Let's suppose that the common physics of the NLS1 phenomenon is captured by the Eddington ratio. The Hβ line width is given by the virial equation $\Delta V \propto (M_{\mathrm{BH}}/R_{\mathrm{BLR}})^{1/2}$. From the R–L relationship of the last section and the definition of the Eddington ratio $\dot{m} = \dot{M}/\dot{M}_{\mathrm{Edd}} \propto \dot{M}/M_{\mathrm{BH}}$, we see that the dependence of the line width is

$$\Delta V \propto \left(\frac{M_{\mathrm{BH}}}{L_{\mathrm{AGN}}^{1/2}} \right)^{1/2} \propto \left(\frac{M_{\mathrm{BH}}}{\dot{M}^{1/2}} \right)^{1/2} \propto \left(\frac{M_{\mathrm{BH}}}{\dot{m}} \right)^{1/4}. \tag{4.1}$$

What this tells us is that for a fixed Eddington ratio $\dot{m}$, the emission lines are broader for more massive black holes. If this is correct, then we should be modifying our definition somewhat, since higher mass black holes will have broader lines even though the Eddington ratio is fixed [84, 32]. Rather than modify the NLS1 definition, I'll just define (arbitrarily) a larger class of "high Eddington ratio sources (HERS)" as those with

$$\Delta V \leq \left(\frac{M_{\mathrm{BH}}}{10^7 M_\odot} \right)^{1/4} 2000\,\mathrm{km\ s^{-1}}. \tag{4.2}$$

The HERS are highlighted in Figure 2b. If the NLS1s are a high Eddington ratio phenomenon, then they are the low-luminosity subset of the larger HERS class. But taken as a group, they do not stand out from the other objects in any properties except line width and profile and the parameters derived directly from these parameters; this is consistent with Bentz [5], but rather at odds with the results of other investigations (see §4.3).

The bottom line is probably that NLS1s are yet another "mixed bag" (cf. [101]) of sources that include both high Eddington rate accretors and low-inclination AGNs. Inclination effects are clearly present, as are some NLS1 characteristics that cannot be explained away as inclination
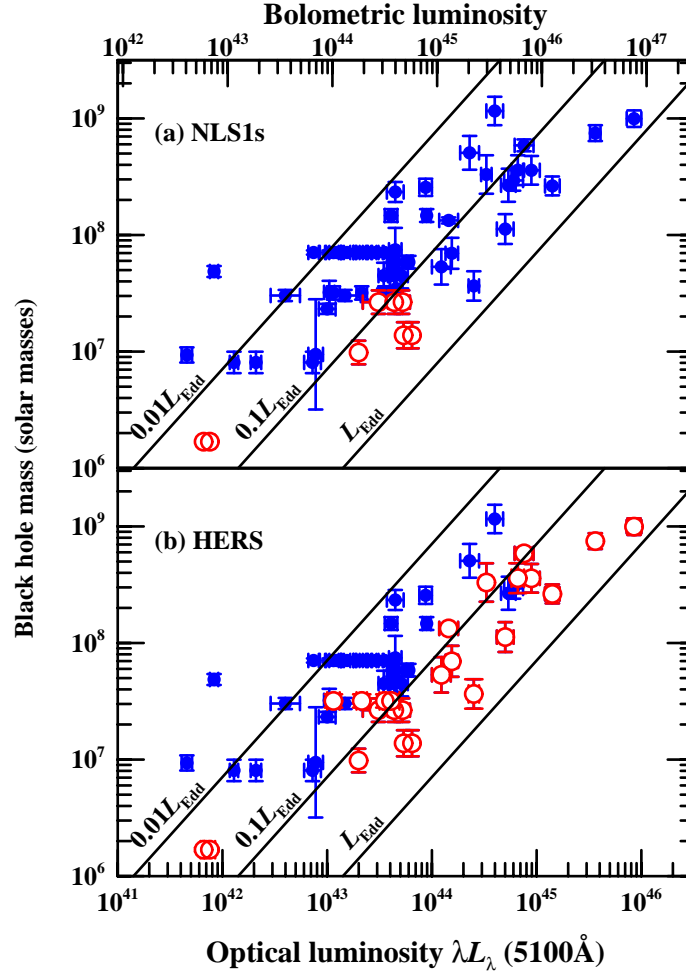
Figure 2: M_{BH}–L_{AGN} for the reverberation-mapped AGNs. Lines of constant Eddington ratio are shown for $\dot{m} = 0.01$, $\dot{m} = 0.10$ and $\dot{m} = 1.0$. Multiple L_{AGN} values for a fixed M_{BH} indicate multiple reverberation results for some sources (notably NGC 5548 at $\sim 7 \times 10^7 M_\odot$). The upper scale shows bolometric luminosity based on a nominal correction $L_{bol} = 9\lambda L_{AGN}$. In the upper panel, NLS1s are shown as open cirles. In the lower panel, high Eddington rate sources (HERS) are shown as open circles.

effects. Indeed, the case can be made that many NLS1s are actually *both* pole-on *and* have high Eddington ratios [17].

4.2 Characterizing the Line Width

So far we have side-stepped the question of what is the better measure of the line width, FWHM or σ_{line}? In this case, "better" means which measure, if either, gives a black hole mass that is unbiased. It is inescapable that at least one of these measures will introduce a bias into the mass scale because the *shape* of AGN emission lines is a function of their width. This is illustrated in Figure 3, which shows FWHM/σ_{line} as a function of FWHM, where again we have highlighted the HERS. Clearly the choice of which measure we use for computing the masses is important. This is illustrated very clearly in Figure 4, which shows a direct comparison of black hole masses based
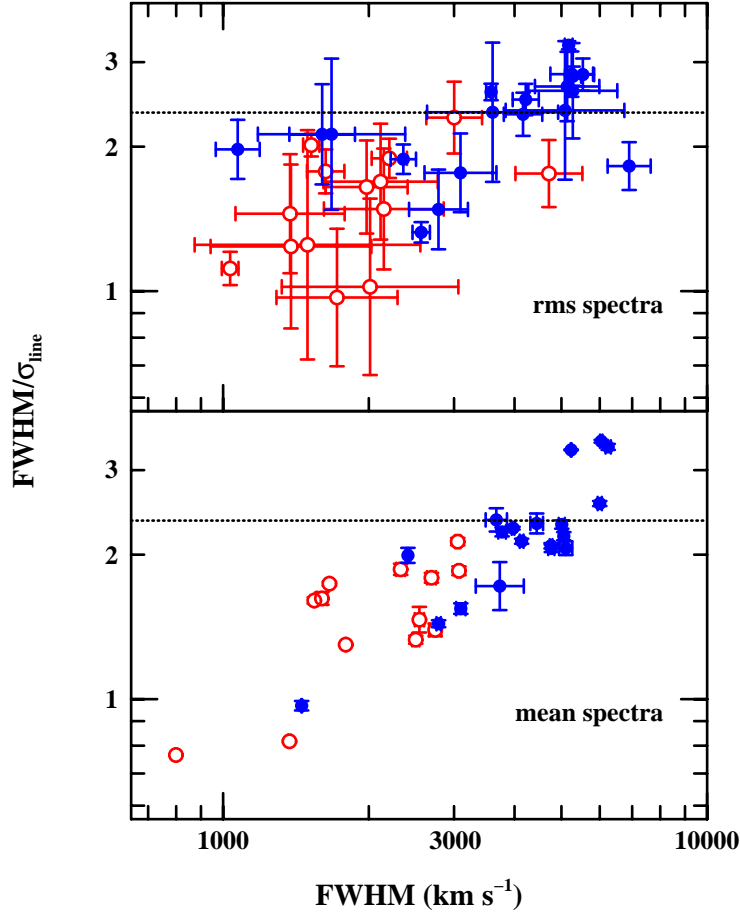
Figure 3: The line-width ratio FWHM/σ_{line} as a function of FWHM for the Hβ line in the rms (top) and mean (bottom) spectra of reverberation-mapped AGNs. In both panels, a dotted line shows the value for a Gaussian profile, FWHM/$\sigma_{\text{line}} = 2.35$. HERS are shown as open circles.

on FWHM with those based on σ_{line}; the HERS have smaller masses for FWHM than for σ_{line} and vice versa for the remainder of the AGNs.

An argument can be made that σ_{line} is the less-biased line-width measure, at least in the case of lines measured in rms spectra [82, 18], the variable part of the spectrum. However, in individual spectra of AGNs, generally the line wings are badly blended with other features, and introduces systematic errors that are a function of line width [26], but the errors introduced are still smaller than the systematic differences that arise from using FWHM instead of σ_{line}.

The clear trend illustrated in Figure 3 demonstrates that it is possible to correct FWHM to σ_{line}; this was, in fact, explicitly proposed by Collin et al. [18]. There are other formulations that have suggested that the dependence on line width in equation (2.1) should be written as FWHM$^{\gamma}$, where γ is a free parameter, which in practice turns out to have a value slightly smaller than two [99]; in essence, this is making the same correction between FWHM and σ_{line}, since the latter is what was used to compute the reverberation-based masses [82].

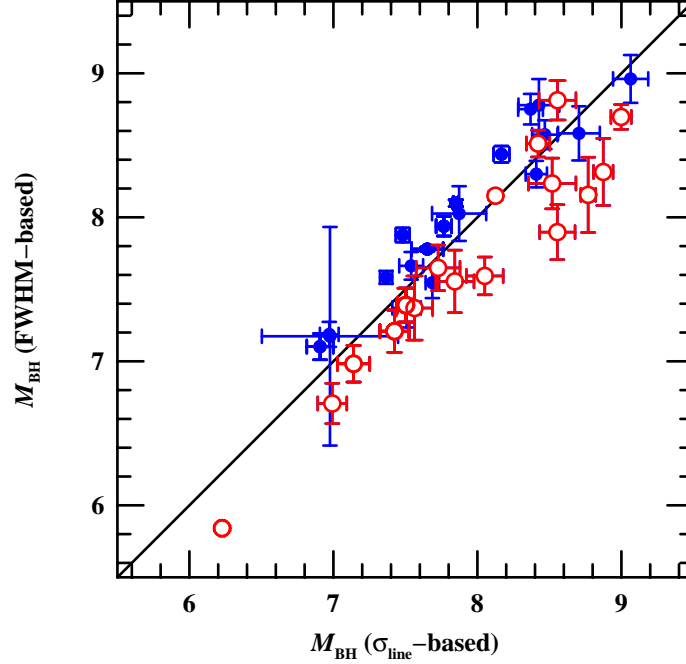It is important to sort this out as incorrect parameterizations will give misleading results. While

Figure 4: A direct comparison of black hole masses based on different line-width measures, FWHM and the line dispersion σ_{line}, in both cases based on measurement of the Hβ line in the rms spectrum. HERS are shown as open circles. Relative to σ_{line}, FWHM yields lower masses for HERS because of the higher kurtosis of the Balmer-line profiles in HERS spectra.

the issue has not been completely resolved at this point, there is a current controversy that in any case illustrates the point. Steinhardt & Elvis [92] show that if one plots black-hole mass versus AGN luminosity for the SDSS DR5 quasars, in each redshift bin it is found that while the lower-mass AGNs approach the Eddington limit, the higher mass AGNs do not. In other words, the axis of the distribution of quasars on the L_{AGN}–M_{BH} diagram (similar to Figure 2, with the axes interchanged), does not run parallel to lines of constant $\dot{m}$, but is rather more shallow. The absence of higher mass AGNs with high values of the Eddington ratio is referred to as the "sub-Eddington boundary." The mass measurements used by Steinhardt & Elvis are from Shen et al. [90], in which the emission lines were fit with a pair of Gaussians, one for the narrow component and one for the broad component, and the black hole mass was computed using equation (2.1) with the FWHM measurement for the broad-component best-fit Gaussian. In an independent study, Rafiee & Hall [85] went back to the original DR5 spectra and measured σ_{line} from the original data. When they use σ_{line} to compute the black hole masses, they find that the sub-Eddington boundary disappears, and that in each redshift range the distribution of AGNs in the L_{AGN}–M_{BH} diagram is along constant values of $\dot{m}$. This, of course, does not prove that the sub-Eddington boundary is an artifact of how the line widths were characterized, but it is certainly suggestive since the Rafiee & Hall result seems intuitively more likely to be correct. Indeed, Figures 3 and 4 show that using FWHM instead of σ_{line} will certainly lead to overestimating the masses of AGNs with the broadest lines and underestimating the masses of the AGNs with the narrowest lines, which would produce

exactly the sub-Eddington boundary phenomenon. A Gaussian fit (*rarely* a good description of a broad-line profile) will have the same effect (see Figure 3), so it's not immediately clear whether the problem is principally the Gaussian assumption or the use of FWHM.

Is the sub-Eddington boundary real? Perhaps. But I doubt it.

4.3 Host-Galaxy Properties

Currently the reverberation-based mass scale relies heavily on correlations between black hole mass and host-galaxy properties. It is explicitly assumed that these relationships are the same in active and quiescent galaxies. A particular concern is the nature of the M_{BH}–σ_* relationship, which currently provides the zero-point calibration for the reverberation mass scale. Batcheldor [4] has argued that the M_{BH}–σ_* relationship is a selection effect caused by preferentially observing sources with a resolvable radius of influence (equation 1.1), though Gültekin et al. [45] disagree. Indeed, the existence of an AGN M_{BH}–σ_* relationship also argues against this as a selection effect, since there is only a subtle radius-of-influence bias in the AGN sample[3].

There is also active discussion about the host galaxies of NLS1s and whether or not there are differences between these and the hosts of other AGNs. Crenshaw, Kraemer, & Gabel [20] claimed that NLS1 hosts are disproportionately barred galaxies, and larger samples seem to confirm this [71]. This raises concerns as there is evidence [40] that the M_{BH}–σ_* relationship is different for barred galaxies than for non-barred and elliptical galaxies. There are also indications that the hosts of NLS1s have pseudo-bulges rather than classical bulges [66, 74, 65, 75], and pseudo-bulges might [5] or might not [48] not follow the M_{BH}–σ_* relationship. This is a potential problem not only for the overall reverberation-mapping mass scale, but for the *relative* masses of NLS1s compared to other AGNs.

4.4 Toward Higher Precision Masses

At the present time, the masses that can be obtained from single-epoch spectra are probably accurate to about the 0.5 dex level, but we start to see hints of bias in the mass scale at this point. Proper characterization of line widths in individual (single-epoch) spectra is probably the single most significant problem, although this does not seem to be generally appreciated. Beyond this, there are several important questions that need to be addressed as we strive to make better black hole mass measurements, and some of these are addressed in other contributions to these proceedings:

- Are black hole mass/host-galaxy relationships the same in AGNs and quiescent galaxies? Do AGNs and quiescent galaxies differ in incidence of pseudo-bulges, and how does this relate to black hole growth and star-formation rates [86, 87]?

- Are black hole mass/host-galaxy relationships the same in NLS1s (or HERS) as in other AGNs?

- How reliable are the scaling relationships over luminosity and redshift?

---

[3]Specifically, the most luminous objects in the reverberation database were selected at least in part for their apparent brightness, so there is a bias toward HERS, as is well-known for the Palomar–Green sample from which these are drawn.

- Does failure to account for radiation pressure lead us to underestimate $M_{\rm BH}$? NLS1s (or HERS) are the likely testing ground for this because the radiation pressure term in the mass equation [63] will be relatively highest in these sources.

- What problems do we encounter by using different emission lines to determine $M_{\rm BH}$? In particular, there are lingering doubts about the use of C IV, despite good arguments that it is generally a good mass-indicator [30, 95]. My own observation (see also [30, 95]) is that much of the evidence that C IV is problematic is based on data that are too poor to address the issue.

- How can we resolve the inclination/Eddington ratio ambiguity in NLS1s (or HERS)?

Which brings us ...

5. Back to Reverberation Mapping

While we expect that ongoing research will lead toward higher accuracy and higher precision black hole masses, improvements in reverberation mapping is the direct path to address all of our concerns about black hole masses. The velocity–delay map for the Balmer lines in Arp 151 [14] indicates a rich, complex structure and a preliminary velocity–delay map for the NLS1 NGC 4051 [30] suggests that the Balmer-line emitting region in this source is a nearly face-on disk. There are now several data sets of comparable quality [43], so additional velocity–delay maps can be expected in the near future. As more and better velocity–delay maps become available, it will be possible to model the kinematics and geometry of the BLR directly from the reverberation data and thus determine the central black hole masses without recourse to other methods; this is what will be required for reverberation mapping to become a primary method.

The problem with reverberation mapping is, of course, simply that it is both expensive (in terms of telescope time) and risky (since the pattern of variability in a given source is unpredictable). In the future, it will probably be possible to employ more clever strategies for reverberation campaigns, for example, using photometric monitoring from synoptic surveys like LSST to trigger campaigns at opportune times. And given good photometric coverage, spectroscopic monitoring can be sparser and tailored to the goals of the program (for a good example of an opportunistic program, see [3]).

But it remains true that reverberation mapping is currently the *only* way to measure the masses of black holes in galaxies out to cosmologically interesing distances and the only way to probe the low-mass end of the distribution, as illustrated in Figure 5. Even with a diffraction-limited 30-m telescope at H-band, it is impossible to resolve the black hole radius of influence for $M_{\rm BH} < 10^8\,M_\odot$ at the distance of the Coma cluster. Reverberation mapping, by substituting time resolution for angular resolution, can extend direct measurements of black hole masses to much larger distances.
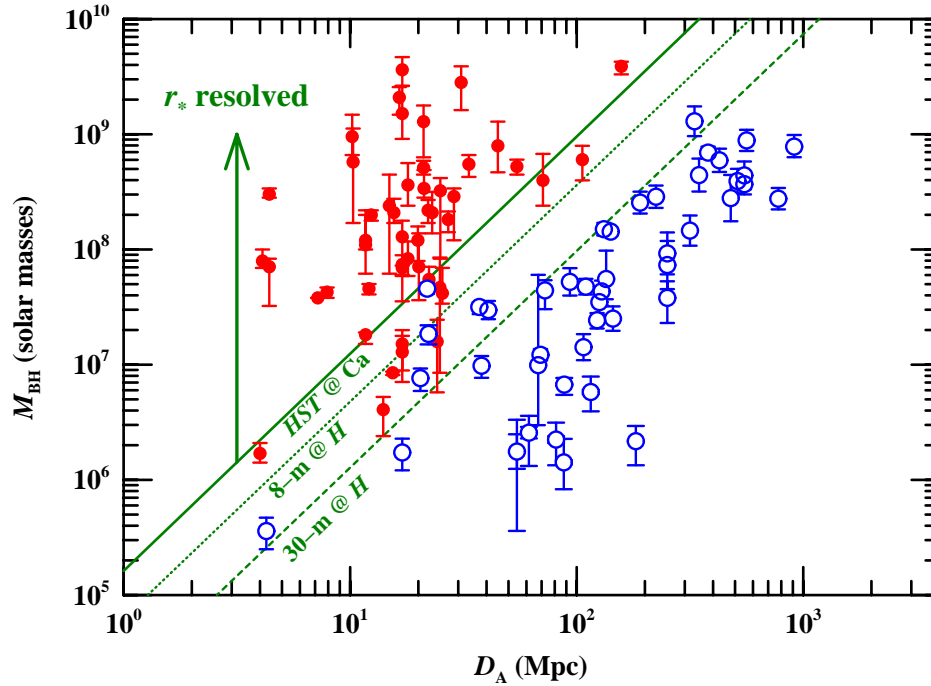
Figure 5: M_{BH} versus luminosity distance for nuclear black holes with direct measurements of their masses. Reverberation-based masses are shown as open circles and masses measured by stellar or gas dynamics are shown as filled circles. The limiting black hole radius of influence as a function of mass is shown for the cases of *Hubble Space Telescope* at the Ca II triplet ($\sim 8600\,\text{Å}$), an 8-m telescope at *H*-band, and a 30-m telescope at *H*-band. A bare handful of AGNs are close enough to resolve the radius of influence and thus measure their black hole masses by the same techniques used on relatively local galaxies.

References

[1] A. A. Abdo *et al.* 2009, *ApJ*, **707**, L142–L147.

[2] J. A. Baldwin, G. J. Ferland, K. T. Korista, & D. Verner 1995, *ApJ*, **455**, L119–L122.

[3] A. J. Barth *et al.* 2011, *ApJ*, **732**, 121–134.

[4] D. Batcheldor 2010, *ApJ*, **711**, L108–L111.

[5] M. Bentz 2011, in *Proceedings of the Workshop Narrow-Line Seyfert 1 Galaxies and Their Place in the Universe*, PoS(NLS1)033.

[6] M. C. Bentz, B. M. Peterson, R. W. Pogge, M. Vestergaard, & C. A. Onken 2006, *ApJ*, **644**, 133–142.

[7] M. C. Bentz, K. D. Denney, E. M. Cackett, M. Dietrich, J. K. J. Fogel, H. Ghosh, K. Horne, C. Kuehn, T. Minezaki, C. A. Onken, B. M. Peterson, R. W. Pogge, V. I. Pronik, D. O. Richstone, S. G. Sergeev, M. Vestergaard, M. G. Walker, & Y. Yoshii 2006, *ApJ*, **651**, 775–781.

 [8] M. C. Bentz, K. D. Denney, E. M. Cackett, M. Dietrich, J. K. J. Fogel, H. Ghosh, K. D. Horne, C. Kuehn, T. Minezaki, C. A. Onken, B. M. Peterson, R. W. Pogge, V. I. Pronik, D. O. Richstone, S. G. Sergeev, M. Vestergaard, M. G. Walker, & Y. Yoshii 2007, *ApJ*, **662**, 205–212.

 [9] M.C. Bentz, J. L. Walsh, A. J. Barth, N. Baliber, N. Bennert, G. Canalizo, A. V. Filippenko, M. Ganeshalingam, E. L. Gates, J. E. Greene, M. G. Hidas, K. D. Hiner, N. Lee, W. Li, M. A. Malkan, T. Minezaki, F. J. D. Serduke, J. H. Shiode, J. M. Silverman, T. N. Steele, D. Stern, R. A. Street, C. E. Thornton, T. Treu, X. Wang, J.-H. Woo, & Y. Yoshii 2008, *ApJ*, **689**, L21–L24.

[10] M. C. Bentz, B. M. Peterson, R. W. Pogge, & M. Vestergaard 2009, *ApJ*, **694**, L166–L170.

[11] M. C. Bentz, B. M. Peterson, H. Netzer, R. W. Pogge, & M. Vestergaard 2009, *ApJ*, **697**, 160–181.

[12] M. C. Bentz *et al.* 2009, *ApJ*, **705**, 199–217.

[13] M. C. Bentz *et al.* 2010, *ApJ*, **716**, 993–1011.

[14] M. C. Bentz *et al.* 2010, *ApJ*, **720**, L46–L51.

[15] R. D. Blandford & C. F. McKee 1982, *ApJ*, **255**, 419–439.

[16] N. G. Bochkarev & C. M. Gaskell 2009, *Ast. Letters*, **35**, 287–293.

[17] T. A. Boroson 2011, in *Proceedings of the Workshop Narrow-Line Seyfert 1 Galaxies and Their Place in the Universe*, `PoS(NLS1)003`.

[18] S. Collin, T. Kawaguchi, B. M. Peterson, & M. Vestergaard 2006, *A&A*, **456**, 75–90.

[19] D. M. Crenshaw, T. C. Fischer, S. B. Kraemer, & H. R. Schmitt 2011, in *Proceedings of the Workshop Narrow-Line Seyfert 1 Galaxies and Their Place in the Universe*, `PoS(NLS1)027`.

[20] D. M. Crenshaw, S. B. Kraemer, & J. R. Gabel 2003, *AJ*, **126**, 1690–1698.

[21] K. Davidson 1972, *ApJ*, **171**, 213–231.

[22] K. Davidson & H. Netzer 1979, *Rev. Mod. Phys.*, **51**, 715–766.

[23] R. I. Davies *et al.* 2006, *ApJ*, **646**, 754–773.

[24] R. Decarli, M. Dotti, F. Haardt, & S. Zibetti 2011, in *Proceedings of the Workshop Narrow-Line Seyfert 1 Galaxies and Their Place in the Universe*, `PoS(NLS1)041`.

[25] K. D. Denney, M. C. Bentz, B. M. Peterson, R. W. Pogge, E. M. Cackett, M. Dietrich, J. K. J. Fogel, H. Ghosh, K. D. Horne, C. Kuehn, T. Minezaki, C. A. Onken, V. I. Pronik, D. O. Richstone, S. G. Sergeev, M. Vestergaard, M. G. Walker, & Y. Yoshii 2006, *ApJ*, **653**, 152–158.

[26] K. D. Denney, B. M. Peterson, M. Dietrich, M. Vestergaard, & M. C. Bentz 2009, *ApJ*, **692**, 246–264.

[27] K. D. Denney *et al.* 2009, *ApJ*, **702**, 1353–1366.

[28] K. D. Denney *et al.* 2009, *ApJ*, **704**, L80–L84.

[29] K. D. Denney *et al.* 2010, *ApJ*, **721**, 715–737.

[30] K. D. Denney *et al.* 2011, in *Proceedings of the Workshop Narrow-Line Seyfert 1 Galaxies and Their Place in the Universe*, `PoS(NLS1)034`.

[31] E. A. Dibai 1977, *Soviet Astronomy*, **3**, 1–3.

[32] D. Dultzin. M. L. Martínez, P. Marziani, J. W. Sulentic, & A. Negrete 2011, in *Proceedings of the Workshop Narrow-Line Seyfert 1 Galaxies and Their Place in the Universe*, `PoS(NLS1)012`.

[33] G. J. Ferland, K. T. Korista, & B. M. Peterson 1990, *ApJ*, **363**, L21–L25.

[34] L. Ferrarese & D. Merritt 2000, *ApJ*, **539**, L9–L12.

[35] L. Ferrarese, R. W. Pogge, B. M. Peterson, D. Merritt, A. Wandel, & C, L. Joseph 2001, *ApJ*, **555**, L79–L82.

[36] S. Fine *et al.* 2008, *MNRAS*, **390**, 1413–1429.

[37] L. Foschini 2011, in *Proceedings of the Workshop Narrow-Line Seyfert 1 Galaxies and Their Place in the Universe*, `PoS(NLS1)024`.

[38] K. Gebhardt *et al.* 2000, *ApJ*, **539**, L13–L16.

[39] K. Gebhardt *et al.* 2000, *ApJ*, **543**, L5–L8.

[40] A. W. Graham, C. A. Onken, E. Athanassoula, & F. Combes 2011, *MNRAS*, **412**, 2211–2228.

[41] J. E. Greene *et al.* 2010, *ApJ*, **723** 409–416.

[42] C. J. Grier *et al.* 2008, *ApJ*, **688**, 837–843.

[43] C. J. Grier, B. M. Peterson, K. D. Denney, P. Martini, R. W. Pogge, & M. C. Bentz 2011, in *Proceedings of the Workshop Narrow-Line Seyfert 1 Galaxies and Their Place in the Universe*, `PoS(NLS1)052`.

[44] K. Gültekin, D. O. Richstone, K. Gebhardt, T. R. Lauer, S. Tremaine, M. C. Aller, R. Bender, A. Dressler, S. M. Faber, A. V. Filippenko, R. Green, L. C. Ho, J. Kormendy, J. Magorrian, J. Pinkney, & C. Siopis 2009, *ApJ*, **698**, 198–221.

[45] K. Gültekin, S. Tremaine, A. Loeb, & D. O. Richstone 2011, *ApJ*, in press [arXiv:1106.1079]

[46] E. K. S. Hicks & M.A. Malkan 2008, *ApJS*, **174**, 31–73.

[47] K. Horne, B. M. Peterson, S. J. Collier, & H. Netzer 2004, *PASP*, **116**, 465–476.

[48] J. Hu 2007, *MNRAS*, **386**, 2242–2252.

[49] M.J. Jarvis & R.J. McLure 2006, *MNRAS*, **369**, 182–188.

[50] S. Kaspi, P. S. Smith, H. Netzer, D. Maoz, B. T. Jannuzi, & U. Giveon 2000, *ApJ*, **533**, 631–649.

[51] S. Kaspi, D. Maoz, H. Netzer, B. M. Peterson, M. Vestergaard, & B. T. Jannuzi 2005, *ApJ*, **629**, 61–71.

[52] S. Kaspi, W. N. Brandt, D. Maoz, H. Netzer, D. P. Schneider, & O. Shemmer 2007, *ApJ*, **659**, 997–1007.

[53] B. C. Kelly, J. Bechtold, & A. Siemiginowska 2009, *ApJ*, **698**, 895–910.

[54] A. P. Koratkar & C. M. Gaskell 1991. *ApJ*, **370**, L61–L64.

[55] K. T. Korista, J. A. Baldwin, G. Ferland, & D. Verner 1997, *ApJS*, **108**, 401–415.

[56] J. H. Krolik & C. F. McKee 1978, *ApJS*, **37**, 459–483.

[57] C. A. Kuehn, J. A. Baldwin, B. M. Peterson, & K. T. Korista 2008, *ApJ*, **673**, 69–77.

[58] W. Kollatschny 2003, *A&A*, **407**, 461–472.

[59] W. Kollatschny 2003, *A&A*, **412**, L61–L64.

[60] S. Kozłowski *et al.* 2010, *ApJ*, **708**. 927–945.

[61] J. Magorrian, S.Tremaine, D. Richston, R. Bender, G. Bower, A. Dressler, S. M. Faber, K. Gebhardt, R. Green, C. Grillmair, J. Kormendy, & T. Lauer 1999, *AJ*, **115**, 2285–2305.

[62] A. Marconi, D. J. Axon, R. Maiolino, T. Nagao, G. Pastorini, P. Pietrini, A. Robinson, & G. Torricelli 2008, *ApJ*, **678**, 693–700.

[63] A. Marconi 2011, *Proceedings of the Workshop Narrow-Line Seyfert 1 Galaxies and Their Place in the Universe*, PoS(NLS1)040.

[64] W. G. Mathews & E. R. Capriotti 1984, in *Astrophysics of Active Galaxies and Quasi-Stellar Objects*, ed. J. S. Miller (Mill Valley: University Science Books), pp. 185–233.

[65] S. Mathur 2011, in *Proceedings of the Workshop Narrow-Line Seyfert 1 Galaxies and Their Place in the Universe*, PoS(NLS1)035.

[66] S. Mathur, D. Fields, B. M. Peterson, & D. Grupe 2011, submitted to *ApJ* [arXiv:1102.0537]

[67] C. F. McKee & B. Tarter 1975, *ApJ*, **202**, 306–318.

[68] R. J. McLure & M. J. Jarvis 2002, *MNRAS*, **337**, 109–116.

[69] K. G. Metzroth, C. A. Onken, & B. M. Peterson 2006, *ApJ*, **647**, 901–909.

[70] C. H. Nelson, R. F. Green, G. Bower, K. Gebhardt, & D. Weistrop 2004, *ApJ*, **615**, 652–661.

[71] K. Ohta, K. Aoki, T. Kawaguchi, & G. Kiuchi 2007, *ApJS*, **169**, 1–20.

[72] C. A. Onken, L. Ferrarese, D. Merritt, B. M. Peterson, R. W. Pogge, M. Vestergaard, & A. Wandel 2004, *ApJ*, **615**, 645–651.

[73] C. A. Onken *et al.* 2007, *ApJ*, **670**, 105–115.

[74] G. Orban de Xivry, R. Davies, M. Schartmann, S. Komossa, A. Marconi, E. Hicks, H. Engel, & L. Tacconi 2011, submitted to *MNRAS* [arXiv:1104.5023]

[75] G. Orban de Xivry, R. Davies, M. Schartmann, S. Komossa, A. Marconi, E. Hicks, H. Engel, & L. Tacconi 2011, in *Proceedings of the Workshop Narrow-Line Seyfert 1 Galaxies and Their Place in the Universe*, PoS(NLS1)035.

[76] B. M. Peterson 1993, *PASP*, **105**, 247–268.

[77] B. M. Peterson, & A. Wandel 1999, *ApJ*, **521**, L95–L98.

[78] B. M. Peterson, & A. Wandel 2000, *ApJ*, **540**, L13–L16.

[79] B. M. Peterson, K. A. Meyers, E. R. Capriotti, C. B. Foltz, B. J. Wilkes, & H. R. Miller 1985, *ApJ*, **292**, 164–171.

[80] B. M. Peterson *et al.* 2000, *ApJ*, **542**, 161–174.

[81] B. M. Peterson *et al.* 2002, *ApJ*, **581**. 197–204.

[82] B. M. Peterson *et al.* 2004, *ApJ*, **613**, 682–699.

[83] B. M. Peterson *et al.* 2005, *ApJ*, **632**, 799–808.

[84] B. M. Peterson 2007, in *The Central Engine of Active Galactic Nuclei*, ed. L. C. Ho & J.-W. Wang, *ASP Conference Series*, **373**, 3–12.

[85] A. Rafiee & P. B. Hall 2011, *MNRAS*, in press [arXiv:1011.1268]

[86] E. Sani, D. Lutz, G. Risaliti, H. Netzer, L. Gallo, B. Trakhtenbrot, E. Sturm, & T. Boller 2010, *MNRAS*, **403**, 1246–1260.

[87] E. Sani, D. Lutz, G. Risaliti, H. Netzer, L. Gallo, B. Trakhtenbrot, E. Sturm & T. Boller 2011, in *Proceedings of the Workshop Narrow-Line Seyfert 1 Galaxies and Their Place in the Universe*, `PoS(NLS1)038`.

[88] S. G. Sergeev, S. A. Klimanov, V. T. Doroshenko, Yu. S. Efimov, S. V. Nazarov, & V. I. Pronik 2011, *MNRAS*, **410**, 1877–1885.

[89] J. C. Shields, G. J. Ferland, & B. M. Peterson 1995, *ApJ*, **441**, 507–520.

[90] Y. Shen, J. E. Greene, M. A. Strauss, G. T. Richards, & D. P. Schneider 2008, *ApJ*, **680**, 169–190.

[91] C. S. Stalin, S. Jeyakumar, R. Coziol, R. .S. Pawase, & S. S. Thakur 2011, *MNRAS*, in press [arXiv:1105.1677]

[92] C. L. Steinhardt & M. Elvis, 2010, *MNRAS*, **402**, 2637–2648.

[93] M. Vestergaard 2002, *ApJ*, **571**, 733–752.

[94] M. Vestergaard 2004, *ApJ*, **601**, 676–691.

[95] M. Vestergaard, K. Denney, X. Fan, J. J. Jensen, B. Kelly, P. Osmer, B. M. Peterson, & C. Tremonti in *Proceedings of the Workshop Narrow-Line Seyfert 1 Galaxies and Their Place in the Universe*, `PoS(NLS1)010`.

[96] M. Vestergaard & B. M. Peterson 2005, *ApJ*, **625**, 688–698.

[97] M. Vestergaard & B. M. Peterson 2006, *ApJ*, **641**, 689–709.

[98] A. Wandel, B. M. Peterson, & M. A. Malkan 1999, *ApJ*, **526**, 579–591.

[99] J.-G. Wang, X.-B. Dong, T.-G. Wang, L. C. Ho, W. Yuan, H. Wang, K. Zhang, S. Zhang, & H. Zhou 2009, *ApJ*, **707**, 1334–1346.

[100] D. M. Whittle 1985, *MNRAS*, **213**, 1–31.

[101] R. J. Williams, S. Mathur, & R. W. Pogge 2004, *ApJ*, **610**, 737–744.

[102] B. J. Wills & I. W. A. Browne 1986, *ApJ*, **302**, 56–63.

[103] J. Woo, T. Treu, A. J. Barth, S. A. Wright, J. L. Walsh, M. C. Bentz, P. Martini, V. N. Bennert, G. Canalizo, A. V. Filippenko, E. Gates, J. Greene, W. Li, M. A. Malkan, D. Stern, & T. Minezaki 2010, *ApJ*, **716**, 269–280.

[104] Y. Zu, C. S. Kochanek, & B. M. Peterson 2011, *ApJ*, in press [arXiv:1008.0641]